Metal-insulator transition of the Kagomé lattice fermions at 1/3 filling

Satoshi Nishimoto,[1] Masaaki Nakamura,[2] Aroon O'Brien,[3] and Peter Fulde[3,4]

[1]*Leibniz-Institut für Festkörper- und Werkstoffforschung Dresden, D-01171 Dresden, Germany*
[2] *Department of Physics, Tokyo Institute of Technology, Tokyo 152-8551, Japan*
[3] *Max-Planck-Institut für Physik komplexer Systeme, Nöthnitzer Straße 38, D-01187 Dresden, Germany*
[4]*Asia Pacific Center for Theoretical Physics, Pohang, Korea*

(Dated: January 6, 2010)

We discuss the metal-insulator transition of the spinless fermion model on the Kagomé lattice at 1/3-filling. The system is analyzed using exact diagonalization, the density-matrix renormalization group methods and the random phase approximation. In the strong-coupling region, the charge-ordered ground state is consistent with the predictions of the effective model with a plaquette order. We find that the qualitative properties of the metal-insulator transition are totally different depending on the sign of the hopping integrals, reflecting the difference of band structure at the Fermi level.

PACS numbers: 71.10.Hf, 71.27.+a, 71.10.-w

Introduction— For a long time, the exotic phenomena emergent in geometrical frustration have been fascinating but challenging subjects of research in condensed matter physics [1]. An essential difficulty of frustrated systems is attributed to their highly-degenerate ground states in the classical sense. It is common practice to determine how the degeneracy is removed or how the frustration is minimized by adding quantum fluctuations. On a related issue, one of the most intensively studied systems is quantum spins on the Kagomé lattice, which consists of corner-sharing triangles. Very recently, so-called herbertsmithite has been revealed as a promising candidate for an experimental realization of an $S = 1/2$ Kagomé antiferromagnet. Both experimentally [2, 3] and theoretically [4], the low-temperature phase of this system is characterized by a spin liquid state with a small or possibly even no energy gap.

When we turn our attention to itinerant systems on the Kagomé lattice, a greater variety of physical phenomena can be observed. Of particular interest is the competition of distinct ordered states associated with the charge degrees of freedom. From this point of view, an intriguing system is that of 1/3-filled Kagomé lattice fermions. If long-range repulsive interactions are taken into account, there exists a huge number of (nearly) degenerate charge-ordered (CO) states in the strong-coupling regime; a melting of the CO may take place as some ratio of the interaction and hopping.

An experimental candidate to realize this situation is hydrogen-bonded crystals of alkali-hydrosulfates or hydroselenates $M_3H(XO_4)_2$ (M=Cs,Rb,K,Tl, X=S,Se) [5]. These materials exhibit an abrupt change in the electrical conductivity accompanied with a ferroelastic deformation around $T_c = 400$K: above T_c the conductivity within the *a*-*b* plane is very high and it seems to be related to the hopping motion of protons, i.e., super-proton conductivity; below T_c, the protons appear to be localized in some ordering pattern which satisfies the condition that one tetrahedron of XO_4^- has only one hydrogen bond (see Fig. 1). In the regime where only proton ordering is taken into account, an effective model can provide a description of the protons forming the Kagomé network, as discussed later in the paper. Since the number of corner-sharing triangles is equivalent to the number of tetrahedra, the critical behavior in these materials can be described by a metal-insulator transition (MIT) in the Kagomé lattice at 1/3 filling.

Another possible experimental realization may be given by recently developed laser-cooling techniques. It was reported [6] that a two-dimensional optical *trimerized* Kagomé lattice was constructed and that the coupling constants could be controlled using a triple laser beam design. Furthermore, a scheme proposed this year would construct an optical Kagomé lattice at 1/3 filling with the use of just two standing waves and more controllable interactions [7].

Motivated by the optical lattice systems, a model of hard-core bosons on the Kagomé lattice was studied with large scale quantum Monte Carlo simulations and phenomenological dual vortex theory [8, 9]. At 1/3 and 2/3 fillings a weak first-order superfluid-solid transition induced by the nearest-neighbor repulsion was found. Thus, in our work presented here it is natural to consider how this transition occurs in fermion systems. Although the effective model can be shown to be equivalent for hard core bosons and spinless fermions in the strong-coupling limit, features for each, in the weak to intermediate coupling regimes, may differ completely due to the absence of a band picture in boson systems; here the dis-

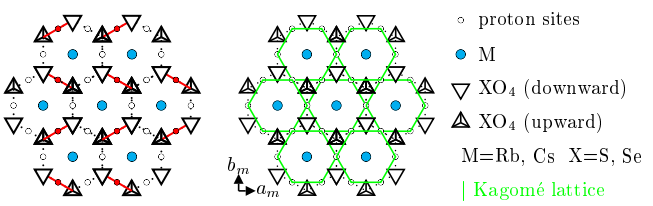

FIG. 1: (Color online) Lattice structure of hydrogen-bonded crystals $M_3H(XO_4)_2$ where the proton sites form the Kagomé lattice (right figure). The left figure presents an example of protons order below the critical temperature. The solid (red) lines denote hydrogen bonds.

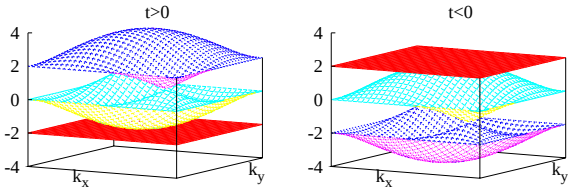

FIG. 2: (Color online) Band structure of the Kagomé lattice fermions for positive (left) and negative (right) hopping energies.

tinction between the two cases is non-trivial.

In this Letter, we therefore study the MIT of the spinless fermion model on the Kagomé lattice at 1/3 filling with the nearest-neighbor repulsive interactions using the exact-diagonalization (ED) and density-matrix renormalization group (DMRG) techniques. Assuming a CO state in the strong-coupling regime, we demonstrate that the nature of the MIT strongly depends on the sign of hopping integral (inversion of the sign corresponds to a switch between $1/3$ and $2/3$ fillings). Lastly, the random phase approximation (RPA) is employed to confirm the numerical results.

Model— The Hamiltonian is

$$\mathcal{H} = t \sum_{\langle i,j \rangle} (c_i^\dagger c_j + \text{H.c.}) + V \sum_{\langle i,j \rangle} n_i n_j, \tag{1}$$

where $c_j^\dagger$ (c_j) is a creation (annihilation) operator of a spinless fermion and n_j ($= c_j^\dagger c_j$) is the corresponding number operator. The repulsive interaction $V(> 0)$ is assumed to act only between neighboring sites $\langle i, j \rangle$. In the non-interacting case $V = 0$, the dispersion relation is given by three bands:

$$\varepsilon(\boldsymbol{k}) = -2t, \quad t\left[1 \pm \sqrt{1 + 8\cos\frac{k_x}{2}\cos\frac{k_y}{2}\cos\left(\frac{k_x - k_y}{2}\right)}\right] \tag{2}$$

(see Fig. 2). It is particularly worth noting that the flat band at 1/3 filling is only filled when $t > 0$. Since the density of states at the Fermi level diverges, the physical properties in the weak- to intermediate-coupling regime are expected to greatly differ from those for $t < 0$. We note that our model with $t > 0$ at $1/3$ filling is equivalent to that with $t < 0$ at $2/3$ filling via the particle-hole transformation.

Let us now consider the case of $t = 0$ with $V > 0$. The nearest-neighbor repulsions V are minimized when each the corner-sharing triangle is occupied by exactly one fermion. This means that the system is in macroscopically degenerate CO state. However, the degeneracy may be lifted when a finite hopping is introduced, and then a CO state with some periodicity must have the lowest energy. The candidates of the CO patterns are quoted in Fig. 3. By looking at the pattern III, one realizes the kinetic energy can be gained through a cyclic hopping process of three fermions on each hexagon. Thus, the lifting takes place with processes of order $|t|^3/V^2$ (lower order contributions, e.g. t^2/V, are the same for all configurations and therefore contribute a constant energy shift rather than lifting the degeneracy). The effective Hamiltonian is derived as [10–12]

$$\mathcal{H}_{\text{eff}} = \frac{12|t|^3}{V^2} \sum_{\text{hexagon}} (c_1^\dagger c_3^\dagger c_5^\dagger c_2 c_4 c_6 + \text{H.c.}), \tag{3}$$

where the sum is over all hexagons on the lattice and the six sites on each hexagon are labeled by 1-6 in a clockwise manner. This is equivalent to the quantum dimer model on the honeycomb lattice which has a plaquette-ordered ground state with three-fold degeneracy [13]. The effective model would be at least qualitatively valid as long as the system is a CO insulator. We note that here the sign of hopping integral has no influence on the physics because the honeycomb lattice has a bipartite structure.

Numerical analysis— First, we compare the lowest energies of each CO pattern to determine if pattern III is indeed stabilized for $V \gg |t| > 0$. We apply the ED technique with periodic boundary conditions. A 12- (18-)site cluster is used to calculate an energy difference $E_{\text{I}} - E_{\text{II}}$ ($E_{\text{II}} - E_{\text{III}}$) [see Fig. 4], where E_{I}, E_{II}, and E_{III} are the energies of the CO patterns I, II, and III, respectively. The periodicity of wave functions is checked in order to identify one CO state from another. As shown in Fig. 5, for both signs of t, E_{III} has the lowest ground-state energy while E_{II} is the second-lowest in the large-V regime; the energy differences are scaled like $E_{\text{II}} - E_{\text{III}} \sim \mathcal{O}(V^{-2})$ and $E_{\text{I}} - E_{\text{II}} \sim \mathcal{O}(V^{-3})$. Since the second-order contributions $\mathcal{O}(|t|/V^2)$ cancel in the energy differences, the behavior of $E_{\text{II}} - E_{\text{III}}$ seems to be consistent with the existence of an energy gain $\mathcal{O}(|t|^3/V^2)$ from the ring exchange process in the effective Hamiltonian (3). As expected, $E_{\text{II}} - E_{\text{III}}$ has no dependence on the sign of t in the large-V region as seen in Fig. 5 (b).

Next, we show that the system indeed exhibits the CO-melting MIT at a finite critical interaction $V = V_{\text{c}}$. To find the MIT critical point, the single-particle gap is calculated using the DMRG method. The DMRG calculation is performed on a $L_x \times L_y$ cluster shown in Fig. 4(b), where the periodic boundary conditions are imposed in the y direction with three unit cells and the open boundary conditions in the x direction

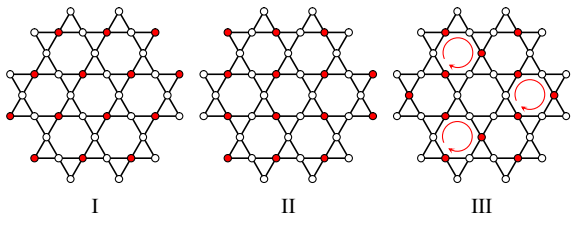

FIG. 3: (Color online) Charge-ordering patterns in the 1/3-filled Kagomé lattice characterized by wave vectors I $(q_{\text{a}}, q_{\text{b}}) = (0, 0)$, II $(0, \pi)$, and III $(2\pi/3, 2\pi/3)$. The circle on pattern III corresponds to the cyclic hopping process by Eq.(3).

with L_x unit cells. We study several lengths of the cluster with up to $L_x = 8$ (78 sites) and extrapolate the finite-size results to the thermodynamic limit $L_x \to \infty$. The single-particle gap is thus given by $\Delta = \lim_{L_x\to\infty} \Delta(L_x)$ with $\Delta(L_x) = E(N_f+1, L_x, L_y) + E(N_f-1, L_x, L_y) - 2E(N_f, L_x, L_y)$, where $E(N_f, L_x, L_y)$ is the ground-state energy of the corresponding cluster with N_f fermions. The upper panels of Figure 6 show the extrapolated values of Δ as a function of V in units of $|t|$. The critical points are estimated as $V_c \sim 2.6$ and 4.0 for $t > 0$ and $t < 0$, respectively. The behaviors of the gap opening are quite different: the gap for $t > 0$ increases almost linearly, while it rises gradually for $t < 0$ like the Berezinskii-Kosterlitz-Thouless transition.

In order to gain further insight, we also calculate the order parameter corresponding to the CO pattern III. The CO phenomenon is observed as a state with a broken translational symmetry: actually, there are two or more degenerate ground states and *one* configuration of the degenerate states is picked out as the ground state by an initial condition of the DMRG calculation, as a consequence of the cylindrical boundary conditions [14]. The order parameter is now defined as the amplitude of the charge-density modulation $\eta(L_x) = n_1 - \frac{1}{2}(n_2 + n_3)$ for a $L_x \times 3$ cluster, where n_1 and n_2 $(= n_3)$ are the charge densities of fermion-rich and fermion-poor sites on a triangle at the center of the cluster. In the lower panels of Figure 6, we show the extrapolated results of order parameter η to the thermodynamic limit, i.e., $\eta = \lim_{L_x\to\infty} \eta(L_x)$, as a function of V. We find that the estimated critical points are almost the same as those obtained from Δ for both signs of t. As seen similarly for Δ., the behavior of η differs markedly depending on the sign of t. For $t > 0$, the transition appears to be nearly discontinuous, which might be analogous to that in a melting MIT observed in hard-core bosons on the triangular lattice [15]; for $t < 0$, it looks continuous, which looks like a weakly first-order phase transition for hard-core bosons on the Kagomé lattice [8]. Hence, we conclude that the criticality for positive t is in stark contrast to that for negative t.

Now, we comment on the difference in values of the MIT critical points between $t > 0$ and $t < 0$. As mentioned above, all the triangles are only allowed to be singly occupied in the

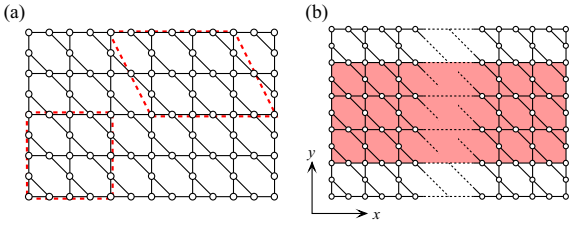

FIG. 4: (Color online) (a) Finite clusters of the Kagomé lattice applied for the ED method. The 12- and 18-site clusters are used to obtain $E_{\rm I} - E_{\rm II}$ and $E_{\rm II} - E_{\rm III}$, respectively. (b) $L_x \times 3$ cluster (shaded regime) for the DMRG method, where the open and periodic boundary conditions are taken for the x and y directions, respectively.

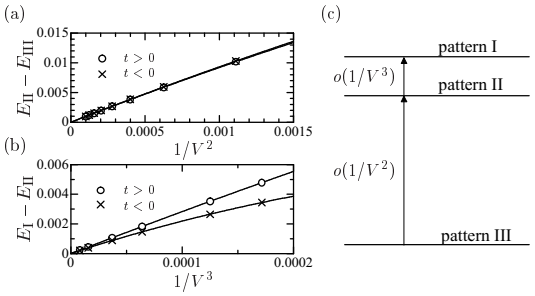

FIG. 5: (Color online) (a) Energy differences $E_{\rm II} - E_{\rm III}$ as a function of $1/V^2$ in units of $|t|$, and (c) $E_{\rm I} - E_{\rm II}$ as a function of $1/V^3$. (c) Relationship of the energies $E_{\rm I}$, $E_{\rm II}$, and $E_{\rm III}$ corresponding to the CO patterns I - III in Fig. 3.

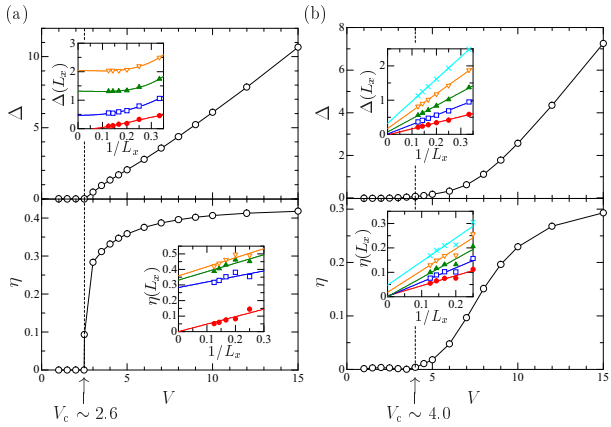

FIG. 6: (Color online) Single-particle gap Δ and order parameter η as a function of the nearest-neighbor repulsion V for (a) positive and (b) negative t values. Insets: Finite-size scaling of each quantity for (a) $V = 2, 3, 4$, and 5; and (b) $V = 2, 3, 4, 5$, and 6, from bottom to top.

CO state. Therefore, our system can be mapped into a single-band half-filled Hubbard model on honeycomb lattice with on-site Coulomb interaction $\mathcal{O}(V)$ if we regard each triangle as a single site. The single-particle gap is then expected to behave like $\Delta \approx V - W_{\rm eff}$ in the large-V region, where $W_{\rm eff}$ is the effective bandwidth. Actually, as seen in Fig. 6, the gap behaves like $\Delta \sim V - 5t$ and $\Delta \sim V - 8|t|$ for $t > 0$ and $t < 0$, respectively. In general, the MIT critical strength is roughly scaled by the bandwidth, i.e., $V_c \propto W_{\rm eff}$. The assumption of the effective bandwidths $W_{\rm eff} = 5t$ for $t > 0$ and $8|t|$ for $t < 0$ are compatible with the obtained critical points. The narrower bandwidth for $t > 0$ might be interpreted as a remnant of the flat band in the noninteracting case [16].

Random phase approximation— In addition, the MIT is investigated analytically using the RPA [17]. The charge susceptibility is given by the Kubo formula as

$$X_{\alpha\gamma}(\boldsymbol{q}, i\omega_l) = \frac{1}{N_{\rm uc}} \int_0^{\beta\hbar} d\tau e^{i\omega_l \tau} \langle n_{\boldsymbol{q},\alpha}(\tau) n_{-\boldsymbol{q},\gamma}(0) \rangle \quad (4)$$

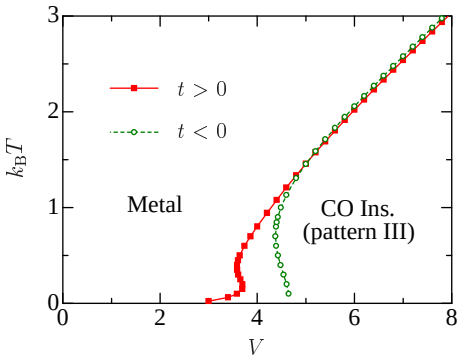

FIG. 7: (Color online) Phase diagram of the 1/3-filled t-V model on the Kagomé lattice obtained by the random phase approximation.

where $\langle \cdots \rangle$ is the ensemble average, $n_{\boldsymbol{q},\alpha}$ is a number operator in momentum space, $\beta = k_{\rm B}T$ is inverse temperature, ω_l is the Matsubara frequency of bosons, and $N_{\rm uc}$ is the number of unit cells. Then, applying the RPA, the charge susceptibility is obtained in the following matrix form,

$$X(\boldsymbol{q}, \imath\omega_l) = \Big[1 + 2v(\boldsymbol{q})X^{(0)}(\boldsymbol{q}, \imath\omega_l))\Big]^{-1} X^{(0)}(\boldsymbol{q}, \imath\omega_l), \quad (5)$$

where the matrix elements of $v(\boldsymbol{q})$ are given by

$$v_{12}(\boldsymbol{q}) = V\cos(q_x/2), \quad v_{13}(\boldsymbol{q}) = V\cos(q_y/2) \quad (6)$$
$$v_{23}(\boldsymbol{q}) = V\cos((q_x - q_y)/2), \quad (7)$$

with the relation $v_{ji} = v_{ij}$ and $v_{ii} = 0$. The bare susceptibility is defined as

$$X(\boldsymbol{q}, \imath\omega_l)^{(0)}_{\alpha\gamma} \equiv \frac{1}{N_{\rm u}} \sum_{\boldsymbol{k}} \sum_{\mu\nu} u^*_{\boldsymbol{k},\alpha\mu} u_{\boldsymbol{k}+\boldsymbol{q},\alpha\nu} u^*_{\boldsymbol{k}+\boldsymbol{q},\gamma\nu} u_{\boldsymbol{k},\gamma\mu} \Gamma(\boldsymbol{k};\boldsymbol{q})^{\mu\nu}_{\omega_l}, \quad (8)$$

where

$$\Gamma(\boldsymbol{k};\boldsymbol{q})^{\mu\nu}_{\omega_l} = \frac{f_{\boldsymbol{k}+\boldsymbol{q},\nu} - f_{\boldsymbol{k},\mu}}{\imath\hbar\omega_l - \varepsilon_{\boldsymbol{k}+\boldsymbol{q},\nu} + \varepsilon_{\boldsymbol{k},\mu}}, \quad (9)$$

with f being the Fermi distribution function. $u_{\boldsymbol{k}}$ is a matrix which diagonalizes the kinetic part of eq. (1) in the momentum space $\boldsymbol{k}$.

The MIT critical point at finite temperature is found by determining the divergence of the diagonal part of eq. (5) for the three sets of CO patterns, I, II, and III. We found that the CO pattern III is always most stable, in agreement with the ED result. The obtained phase diagram is shown in Fig. 7. At high temperature ($k_{\rm B}T/|t| \gg 1$), the MIT phase boundary is almost independent of the sign of t; however, for decreasing temperature the boundaries gradually move apart from each other. The critical points are estimated as $V_{\rm c} \sim 3$ and 4.5 for $t > 0$ and $t < 0$, respectively. These values seem to be not only qualitatively but also quantitatively consistent with those obtained by the DMRG method. It is also interesting that the boundaries show reentrant behaviors.

Conclusion— We study the metal-insulator transition of the spinless fermions on the Kagomé lattice at 1/3-filling using the exact diagonalization, density-matrix renormalization group, and random phase approximation techniques. In the region of large V, the CO pattern in the ground-state is consistent with what is predicted by the ring exchange model. The behaviors of the single-particle gap opening for positive and negative hopping integrals are qualitatively quite different; this is further reflectedin the differing values of the critical point V_c. These differences may arise from the distinct nature of the density of states at the Fermi level in each case. A possible further extension of this work is a consideration of spin degrees of freedom. This is of interest because spins in the CO phase are also frustrated and the configuration is nontrivial.

Acknowledgment— We thank T. Aonuma, G. Fiete, Y. Ohta, and F. Pollmann for very useful discussions. M. N. acknowledges the visitors program at the Max-Planck-Institut für Physik komplexer Systeme, Global Center of Excellence Program "Nanoscience and Quantum Physics" of the Tokyo Institute of Technology by MEXT, and Industrial Technology Research Grant Program in 2005-2008 from the New Energy and Industrial Technology Development Organization (NEDO) of Japan.

[1] R. Moessner and A. P. Ramirez Physics Today, pp. 24, February 2006.
[2] J. S. Helton, K. Matan, M. P. Shores, E. A. Nytko, B. M. Bartlett, Y. Yoshida, Y. Takano, A. Suslov, Y. Qiu, J.-H. Chung, D. G. Nocera, and Y. S. Lee, Phys. Rev. Lett. **98**, 107204 (2007).
[3] P. Mendels, F. Bert, M. A. de Vries, A. Olariu, A. Harrison, F. Duc, J. C. Trombe, J. S. Lord, A. Amato, and C. Baines, Phys. Rev. Lett. **98**, 077204 (2007).
[4] P. Sindzingre and C. Lhuillier, arXiv:0907.4164.
[5] H. Kamimura, Y. Matsuo, S. Ikehata, T. Ito, M. Komukae, and T. Osaka, Phys. Stat. Sol. (b) **241**, 61 (2004).
[6] L. Santos, M. A. Baranov, J. I. Cirac, H.-U. Everts, H. Fehrmann, and M. Lewenstein, Phys. Rev. Lett. **93**, 030601 (2004).
[7] J. Ruostekoski, Phys. Rev. Lett. **103**, 080406 (2009).
[8] S. V. Isakov, S. Wessel, R. G. Melko, K. Sengupta, and Y. B. Kim, Phys. Rev. Lett. **97**, 147202 (2006).
[9] K. Sengupta, S. V. Isakov, and Y. B. Kim, Phys. Rev. B **73**, 245103 (2006).
[10] E. Runge and P. Fulde, Phys. Rev. B **70**, 245113 (2004).
[11] P. Fulde and F. Pollmann, Ann. Phys. (Berlin) **17**, 7, 441 (2008).
[12] A. O'Brien, F. Pollmann and P. Fulde, to be published.
[13] R. Moessner, S. L. Sondhi, and P. Chandra, Phys. Rev. B **64**, 144416 (2001).
[14] S. Nishimoto and C. Hotta, Phys. Rev. B **79**, 195124 (2009).
[15] S. Wessel1 and M. Troyer, Phys. Rev. Lett. **95**, 127205 (2005).
[16] D. Poilblanc and H. Tsunetsugu, arXiv:0911.2413v1 (2009).
[17] T. Aonuma and M. Nakamura, Butcherer thesis, Tokyo Univ. of Science (2006).